The Onset of Mixed Convection in a Porous Layer Heated with a Constant Heat Flux

Joung Hwan Park, Tae Joon Chung, and Chang Kyun Choi
School of Chemical and Biological Engineering, Seoul National University, Seoul 151–744, Korea

Min Chan Kim
Dept. of Chemical Engineering, Cheju National University, Cheju 690–756, Korea

DOI 10.1002/aic.10896
Published online May 15, 2006 in Wiley InterScience (www.interscience.wiley.com).

The onset of mixed convection in a fluid-saturated porous layer between two horizontal plates heated from below with a constant heat flux is investigated theoretically. In the present study, the Darcy model is applied and the resulting nonlinear equations are solved by using the finite volume method. In order to analyze the growth behavior of convective instabilities, the local growth rates of mean temperature and its fluctuations are examined. Based on the numerical results, characteristic distances to represent the onset of secondary flow and also the manifestation of mixed convection are clarified to a certain degree in comparison with available experimental data. The critical distance to mark the onset of intrinsic thermal instability is predicted from a new stability criterion. It is interesting that the propagation theory yields almost the same critical conditions as the numerical ones. © 2006 American Institute of Chemical Engineers *AIChE J,* 52: 2677–2683, 2006
Keywords: onset of mixed convection, porous media, convective instability, local growth rate, critical distance

Introduction

When the primary laminar flow between two horizontal plates is heated from below, secondary flow can set in due to buoyancy forces. In order to control flow and heat transfer, it is important to predict wherefrom the secondary motion sets in. The related mixed convection phenomena often occur in fluid-saturated porous layers, which are encountered in packed-bed processes, geothermal engineering, nuclear reactors, and insulation of buildings. Most of these processes involve nonlinear, developing temperature profiles. To predict the stability criteria in such developing temperature fields, several theoretical models have been suggested.

For the fluid-saturated porous layer with primary laminar flow, Combarnous and Bia[1] investigated the onset of vortex rolls experimentally and reported that with increasing Péclet number, the transverse rolls are changed to the longitudinal rolls aligned to the streamwise direction. Jones and Persichetti[2] and Nield[3] obtained the critical Darcy-Rayleigh number as a function of the Péclet number for various boundary conditions. The convective instabilities in porous media with the through-flow were analyzed by Homsy and Sherwood.[4] For laminar boundary-layer flows, Hsu and Cheng[5] conducted scaling analysis and predicted the critical conditions marking the onset of longitudinal vortex rolls. Lee et al.[6] and Chung et al.[7] employed the propagation theory in order to analyze the convective instability in the laminar flow through the porous channel with isothermal boundaries.

The propagation theory is based on the assumption that for simple, diffusive deep-pool systems, the infinitesimal temperature disturbances under linear theory are propagated mainly within the thermal boundary-layer thickness Δ_T and, based on this length scale factor, the self-similar transformation is forced like the classical boundary-layer theory. This model yields reasonable stability criteria in diffusive fluid layers[8-13] and also

Correspondence concerning this article should be addressed to C. K. Choi at ckchoi@snu.ac.kr.

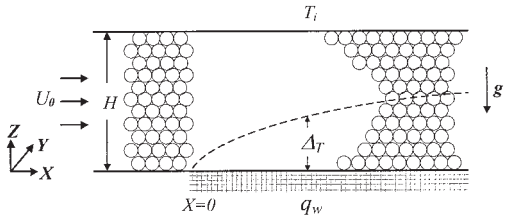

Figure 1. System considered here.

in laminar forced-convection flow systems,[14,15] but it lacks justification.

In the present study the onset of vortex instability in the thermal entrance region of the fluid-saturated horizontal porous layer with a primary laminar forced-convection flow is analyzed for the case of constant-flux heating, as shown in Figure 1. In such thermally developing systems, to understand the local behavior of convective instability two characteristic distances in the streamwise direction are important. The first one is the onset distance of convective instability, that is, intrinsic instability, X_c. For $X \geq X_c$, instabilities grow until manifest convection is observed. The second one is the undershoot distance X_u at which the minimum Nusselt number is exhibited in the plot of the Nusselt number vs. distance. This characteristic distance is frequently used as the distance to mark first manifestation of mixed convection because first detection of secondary flow is not well-defined both theoretically and experimentally. For porous layers, Lai and Kulacki[16] experimentally obtained the average Nusselt numbers for various Darcy-Rayleigh and Péclet numbers. They also considered the size of the heat source and their experimental results were compared to their previous work.[17,18]

In the present study, the critical distance X_c will be predicted with the propagation theory and the resulting prediction will be compared with the numerical simulation using the Boussinesq equation. In the latter nonlinear simulation, we will employ the finite volume method (FVM) to examine the local behavior of instabilities and will predict the characteristic distances to mark the onset of regular vortex rolls, X_c and X_u. These predicted values will be compared with the experimental data of Lai and Kulacki.[16] For this purpose a new stability criterion based on the temperature growth rates is suggested.

Onset of Mixed Convection

Governing equations

The system considered here is a fluid-saturated porous layer with fully-developed laminar flow of uniform velocity U_0 (see Figure 1). The porous layer is confined between two horizontal plates of depth H. The bottom plate is heated with a constant heat flux q_w and the top plate is kept at a constant inlet temperature T_i. For a high q_w, in the thermal entrance region of the laminar flow, the nonlinear temperature profiles develop. For the streamwise distance $X > 0$, the thermal boundary-layer thickness Δ_T increases with increasing X and the buoyancy-driven secondary flow will set in at a certain distance in the form of regular longitudinal vortex rolls. The dimensionless governing equations are expressed under the Boussinesq approximation and Darcy flow:

$$\bar{\nabla} \cdot \boldsymbol{v} = 0, \tag{1}$$

$$\boldsymbol{v} = -\bar{\nabla} p + Ra_D \theta \boldsymbol{k}, \tag{2}$$

$$\partial\theta/\partial x + (\boldsymbol{v} \cdot \bar{\nabla})\theta = \bar{\nabla}^2 \theta, \tag{3}$$

with the boundary conditions,

$$w = 0,\ \partial\theta/\partial z = -1 \qquad \text{at } z = 0, \tag{4a}$$

$$w = \theta = 0 \qquad \text{at } z = 1, \tag{4b}$$

where $\boldsymbol{v}(=\boldsymbol{j}v + \boldsymbol{k}w)$, $p(=PK/(\mu\alpha_e))$, $\theta(=k_e(T - T_i)/(q_w H))$, and $x(=X/(PeH))$ are the dimensionless forms of the Y- and the Z-velocity vector, the pressure P, the temperature T, and the streamwise distance X, respectively. Here K, μ, α_e, k_e, and $Pe(=U_0 H/\alpha_e)$ denote the permeability, the viscosity, the effective thermal diffusivity, the effective thermal conductivity, and the Péclet number, respectively. The dimensionless two-dimensional Cartesian coordinates (y, z) indicate, respectively, the spanwise and the vertical distance with the scale H. The vector differential operator $\bar{\nabla}$ denotes $\boldsymbol{j}\partial/\partial y + \boldsymbol{k}\partial/\partial z$ and $(\boldsymbol{j}, \boldsymbol{k})$ is the horizontal and the vertical unit vector. The important parameter describing the present porous layer, the Darcy-Rayleigh number, is defined as $Ra_D = g\beta q_w K H^2/(k_e \alpha_e \nu)$ where g, β, and ν represent the gravitational acceleration constant, the thermal expansion coefficient, and the kinematic viscosity, respectively. The roll-type instability is observed for $Pe > 0.75$.[1] The numerical results of Prasad et al.[18] show that longitudinal vortex rolls appear for $Pe > 1$. Therefore, we consider only the onset of regular roll-type vortex instability, and the effect of the Prandtl number is neglected with the Darcy model.

In the present system, mixed convection exists for $Ra_D \geq 27.1$. The critical value $Ra_{D,c} = 27.1$ is the well-known value at the thermally fully-developed state.[2,19,20] But in the thermal entrance region with $Ra_D \gg 27.1$, the stability problem becomes complicated. In this study the critical conditions to mark the onset of secondary flow will be analyzed by using both the propagation theory and the numerical simulation. For this purpose a new stability criterion is suggested here, based on the growth rates of disturbances.

Local growth rates

Under mixed convection the velocity and temperature fields are divided into the mean quantities in the y-direction and their fluctuations as usual:

$$\boldsymbol{v} = \langle \boldsymbol{v} \rangle + \boldsymbol{v}', \tag{5}$$

$$\theta = \langle \theta \rangle + \theta', \tag{6}$$

where $\langle\cdot\rangle$ and $'$ represent the mean quantities and their fluctuations, respectively. The mean quantity is a function of x and z.

In the present system, the local buoyancy force in mixed convection is represented by

$$F_B = \rho_i g \beta |T - T_i|, \tag{7}$$

which is produced by temperature variations. Its mean and fluctuation components are $(F_{B,0}, F_{B,1}) = (\langle\theta\rangle, \theta')\rho_i g\beta q_w H/k_e$, where $F_B = F_{B,0} + F_{B,1}$ and ρ_i is the fluid density at $T = T_i$. It is stated that buoyancy-driven convection is driven due to change in temperature. In order to examine the local behavior of thermal instabilities, the following local growth rates of temperature are defined:

$$r_{0,T} = \frac{1}{\langle\theta\rangle_{rms}} \frac{d\langle\theta\rangle_{rms}}{dx}, \tag{8}$$

$$r_{1,T} = \frac{1}{\theta'_{rms}} \frac{d\theta'_{rms}}{dx}, \tag{9}$$

where $r_{0,T}$ and $r_{1,T}$ are, respectively, the local growth rates of the mean temperature and its fluctuations. The subscript *rms* refers to the root-mean-square quantity, that is, $(\cdot)_{rms} = \sqrt{(\int_S (\cdot)^2 dS)/S}$ with $dS = dydz$, where S represents the vertical area at each x. Also, we define the local growth rate of velocity fluctuations as follows:

$$r_{1,V} = \frac{1}{\boldsymbol{v}'_{rms}} \frac{d\boldsymbol{v}'_{rms}}{dx}, \tag{10}$$

where $\boldsymbol{v}'_{rms} = [\int_S (v'^2 + w'^2) dS/S]^{1/2}$.

Local behaviors of convective instability

In the present distance-dependent instability problem, the selection of the inlet conditions is very important. But we do not know what they are and wherefrom they are initiated. It has been thought that thermal noises trigger instabilities. Among them a most energetic, fastest growing mode of disturbances would appear at $x = x_c$, which denotes the critical distance to mark the onset of regular longitudinal vortex rolls. We assume that fluctuations have the following periodic patterns:

$$[\theta', \boldsymbol{v}'] \cong [A(x)\theta_*(z), B(x)\boldsymbol{v}_*(z)]\exp[i(ay)] \quad \text{for } 0 \le x \le x_c, \tag{11}$$

where a is the wavenumber with $i = \sqrt{-1}$. Here A and B are the magnitudes of fluctuations, and the functions θ_* and $\boldsymbol{v}_*$ represent the normalized temperature and velocity amplitudes, respectively.

The critical condition of the onset of intrinsic instability is suggested here:

$$r_{1,T} = r_{0,T} \qquad \text{with } r_{1,V} \ge 0 \qquad \text{at } x = x_c. \tag{12}$$

This means that a fastest growing mode of vortex instability with the wavenumber $a = a_c$ sets in at the smallest distance x_c and it is driven thermally due to temperature fluctuations. It is noted that the condition of $r_{1,V} \ge 0$ ensures the onset of secondary flow and its subsequent growth. For $x < x_c$, magnitudes of fluctuations are very small in comparison with those of primary flow and, therefore, secondary flow is neglected. For $x > x_c$, buoyancy-driven instabilities can grow and secondary flow is detected downstream. Hereafter magnitude of fluctuations is comparable to that of the primary flow. Therefore, the system is assumed stable with $r_{1,T} < r_{0,T}$ but unstable with $r_{1,T} > r_{0,T}$. A stability criterion similar to Eq. 12 was first suggested by Choi et al.[21] for analyzing the onset of convective instability in a Rayleigh-Bénard problem. Their predictions compare favorably with the results from the propagation theory in non-porous diffusive layers.

In the present study the Nusselt number with the characteristic length H is defined as follows:

$$Nu = \frac{1}{L} \int_L \left(\frac{q_w H}{k_e(T_w - T_i)} \right)_{Z=0} dY, \tag{13}$$

where Y is the spanwise distance and L is the width of the cross-section. With secondary flow, Nu deviates from that of the primary laminar forced convection flow and it shows the minimum at $x = x_u$. This characteristic distance is here called the undershoot distance.

Propagation Theory

The propagation theory is based on the assumption that incipient temperature disturbances are propagated mainly within the thermal boundary-layer thickness Δ_T at the marginal stability condition of $r_{1,T} = r_{0,T}$ (see Eq. 12). Therefore, all the variables and parameters having a length scale are rescaled with Δ_T and the self-similar transformation is forced to obtain the stability criteria. The propagation theory has predicted reasonably well the stability criteria for Rayleigh-Bénard convection and also Marangoni-Bénard convection in the horizontal fluid layers.[8,9,22] This model is applied to the present porous layer, as illustrated below.

For the present porous layer the disturbance equations are obtained by linearizing Eqs. 1-3:

$$\bar{\nabla} \cdot \boldsymbol{v}_1 = 0, \tag{14}$$

$$\boldsymbol{v}_1 = -\bar{\nabla} p_1 + Ra_D \theta_1 \boldsymbol{k}, \tag{15}$$

$$\partial\theta_1/\partial x + w_1(\partial\theta_0/\partial z) = \bar{\nabla}^2\theta_1, \tag{16}$$

with the usual boundary conditions,

$$w_1 = \partial\theta_1/\partial z = 0 \qquad \text{at } z = 0, \tag{17a}$$

$$w_1 = \theta_1 = 0 \qquad \text{at } z = 1, \tag{17b}$$

where $\boldsymbol{v} = \boldsymbol{v}_0 + \boldsymbol{v}_1$, $p = p_0 + p_1$, and $\theta = \theta_0 + \theta_1$. Here the subscripts 0 and 1 denote the basic and perturbed quantities, respectively. Under linear theory $\langle\theta\rangle$ can be replaced by θ_0 and θ' by θ_1. With the scaling analysis based on Eqs. 15 and 16 the relation of $Ra_D \sim \delta_T^{-2}$ is obtained at the marginal state, where the dimensionless thermal boundary-layer thickness $\delta_T = \Delta_T/H \sim x^{1/2}$.

Based on $\delta_T(\propto x^{1/2})$, the perturbed quantities are expressed under the usual normal mode analysis as

$$\begin{bmatrix} v_1(x, y, z) \\ w_1(x, y, z) \\ p_1(x, y, z) \\ \theta_1(x, y, z) \end{bmatrix} = \begin{bmatrix} (x^{n+1/2}/a)\, v^*(\zeta) \\ x^{n+1} w^*(\zeta) \\ x^{n+1/2} p^*(\zeta) \\ x^n \theta^*(\zeta) \end{bmatrix} \exp(iay), \qquad (18)$$

where the superscript * indicates the transformed amplitude functions of disturbances with $\zeta = z/x^{1/2}$. This leads to the reasonable continuity equation independent of a, that is, $v^* + dw^*/d\zeta = 0$ from Eq. 14. With $Ra_D \delta_T^2 =$ constant, the above relations make Eqs. 14-17 be transformed as a function of ζ only. The above scaling satisfies Eqs. 1-3. In order to decide the n-value, Eq. 12 is used. The basic temperature of laminar forced convection, θ_0, is well-known:

$$\theta_0 = 2x^{1/2} \sum_{m=0}^{\infty} \left[(-1)^m \left\{ \text{ierfc}\left(\frac{m}{x^{1/2}} + \frac{\zeta}{2} \right) - \text{ierfc}\left(\frac{m+1}{x^{1/2}} - \frac{\zeta}{2} \right) \right\} \right], \qquad (19)$$

of which boundary conditions are $\theta_0 = 0$ at $x = 0$ and $\theta_0 = 1 - z$ as $x \to \infty$.

Now, Eqs. 14-16 are transformed self-similarly by using Eq. 18 with $n = 1/2$ and x is treated as a parameter. Here the distance x is fixed by letting $\partial(\cdot)/\partial x = 0$ under the frame of amplitude coordinates x and ζ instead of x and z (see Eq. 19), which is the same as Riaz et al.'s[13] approach. The resulting self-similar stability equation for small x of $\delta_T \ll 1$ is

$$[(D^2 - a^{*2})\{D^2 + (\zeta/2) D - (a^{*2} + 1/2)\} + Ra_D^* a^{*2} D\theta_0^*] w^* = 0, \qquad (20)$$

with the boundary conditions,

$$w^* = (D^3 - a^{*2} D) w^* = 0 \qquad \text{at } \zeta = 0, \qquad (21a)$$

$$w^* = (D^2 - a^{*2}) w^* = 0 \qquad \text{as } \zeta \to \infty, \qquad (21b)$$

where $a^* = x^{1/2} a$, $Ra_D^* = x Ra_D$, $D\theta_0^* = x^{-1/2} D\theta_0$, and $D = d/d\zeta$. Here Ra_D^* and a^* have been considered as the eigenvalues and, therefore, the principle of the exchange of stabilities can be applied.

The stability equations are solved numerically by employing the outward shooting method. The proper initial values of Dw^*, $D^2 w^*$ at $\zeta = 0$, and Ra_D^* are assumed and then the stability equation is integrated with the fourth-order Runge-Kutta-Gill method. The initially guessed values are corrected by using the Newton-Raphson iteration. As a result, the minimum values of Ra_D^* can be found for the given critical a^*-value, that is, a_c^*. In other words, the critical distance x_c and the critical wavenumber a_c are found for a given Ra_D. With $n = 1/2$ the relation of $r_{1,T} = r_{0,T}$ is obtained from Eqs. 8, 9, and 19, and the solution of Eq. 20.

In this study the critical distance obtained by the propagation theory is written as x_c^*. For $Ra_D > 100$, the resulting critical conditions are found to be

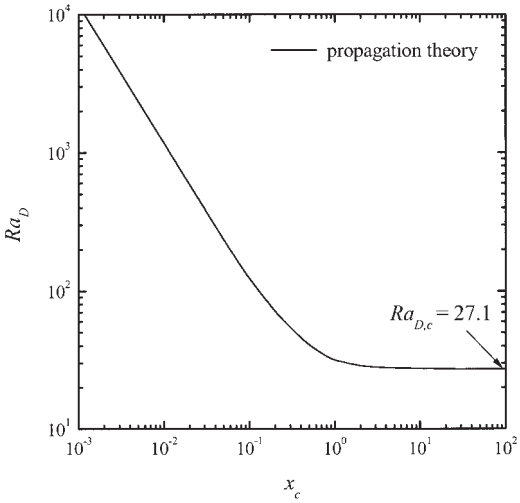

Figure 2. Darcy-Rayleigh number vs. critical distance with a = a_c.

$$Ra_D x_c^* = 11.74, \qquad (22)$$

$$a_c x_c^{*1/2} = 1.007. \qquad (23)$$

The system is considered to be unstable for $x > x_c^*$. Now, the stability criteria are extended to the region of $x \sim 1$ by replacing $\zeta \to \infty$ with $\zeta = 1/x^{1/2}$ in the upper boundary condition (Eq. 21b). The resulting overall stability criteria are shown in Figure 2. It is interesting that the result for large x_c^* approaches the well-known values of $Ra_{D,c} = 27.1$ and $a_c = 2.33$ for $x_c \to \infty$.

Numerical Simulation Procedure

The nonlinear governing equations 1-3 were solved numerically by using the finite volume method FVM.[23] Only one regular longitudinal vortex roll with horizontal periodicity was considered, which represents secondary flow in the horizontally infinite layer. The SIMPLE algorithm was applied to solve the pressure equation, and the hybrid scheme was employed to formulate the convection-diffusion discretization equations. The implicit method was adopted to solve the x-dependent problem and the first-order x-increment was used. The number of meshes was 32×40. Finer meshes were used near the top and bottom boundaries since for a high Ra_D the thermal boundary-layer thickness is very small at small x. Also, to ensure the numerical instability, the distance step $\Delta x = 10^{-6}$ was used. In the present x-dependent problem, the convergence was assumed when the change of the physical quantities was smaller than 10^{-6} at each x-step. The $A(0)$-value was chosen with $0 < A(0) < 10^{-2}$ and the local behaviors of the growth rates represented by Eqs. 8 and 9 were examined.

The inlet conditions at $x = 0$ are constructed as $\theta' = A(0)\theta_*(z)\cos(ay)$, $v' = -B(0)((\partial w_*(z)/\partial z)/a)\sin(ay)$, and $w' = B(0) w_*(z)\cos(ay)$ from Eq. 11, where $A(0)$ and $B(0)$ are the inlet magnitudes. Here it is assumed that for $0 \le x \le x_c$, $\theta_*(z)$ and $w_*(z)$ would not change from the initial patterns and regular longitudinal rolls would appear. This means that the unique disturbance patterns are decided with the converged

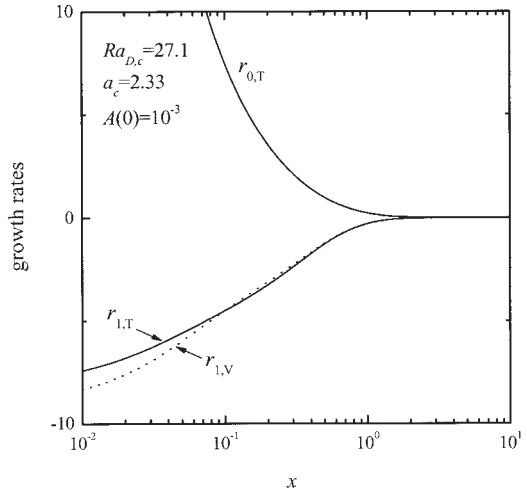

Figure 3. Local growth rates with $Ra_{D,c}$ = 27.1 and a_c = 2.33 for the case of linear temperature profiles.

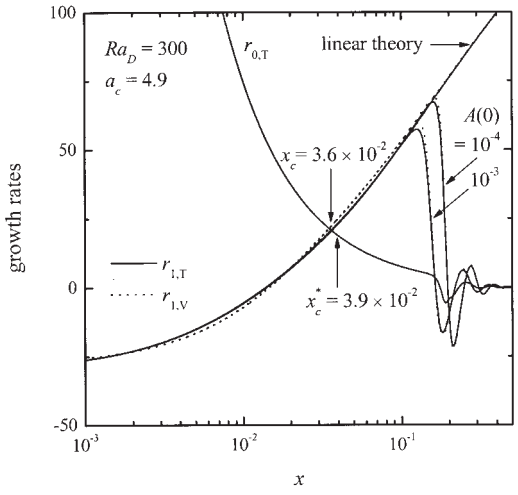

Figure 5. Local growth rates for Ra_D = 300 and a_c = 4.9.

disturbance profiles obtained by iterating the calculation for $0 \leq x \leq x_c$.

Numerical Simulation Results

The results of the numerical simulation by the FVM are reported here. For the case of the linear base temperature, the growth rates ($r_{0,T}$, $r_{1,T}$, and $r_{1,V}$) are illustrated in Figure 3 with its well-known critical conditions of $Ra_{D,c} = 27.1$ and $a_c = 2.33$. It shows the relation of $r_{0,T} = r_{1,T} = r_{1,V} = 0$ as $x \to \infty$. In this limiting case, x_c becomes infinite and it is known that $r_{1,T}$, $r_{1,V} \leq 0$. But for $Ra_D < 27.1$, it is shown that $r_{1,T} < 0$ even if $x \to \infty$. Therefore, it is here verified that the critical Darcy-Rayleigh number $Ra_{D,c}$ is equal to 27.1 and also the present numerical scheme is a reasonable one.

With $Ra_D = 300$ and $A(0) = 10^{-4}$ the behavior of fluctuations along the streamwise distance x is illustrated in Figure 4. For small x, both w'_{rms} and θ'_{rms} retain almost the same magnitudes as their inlet ones. Therefore, numerically given disturbances may set in anywhere in the range of $0 < x \ll x_c$. This supports Mahler and Schechter's[24] viewpoint that initiated thermodynamic disturbances would not grow or decay at their early stage. But in the region of $0.03 < x < 0.2$ they increase sharply with increasing x. The local growth rates are illustrated in Figure 5. The stability condition represented by Eq. 12 yields $x_c = 3.6 \times 10^{-2}$ with $a_c = 4.9$ for $Ra_D = 300$. Here the $r_{1,T}$ - and $r_{1,V}$-paths are the unique ones but the former is almost independent of the inlet velocity condition. The maximum values of $r_{1,T}$ and $r_{1,V}$ appear at $x = x_{m,T}$ and $x = x_{m,V}$, respectively. Up to these distances, the difference between the results from nonlinear equations and those from linear ones is very small. The latter ones start to deviate significantly at $x = x_{m,V}$ from the nonlinear ones, and the superexponential growth of fluctuations is suppressed due to the nonlinear effects. Since secondary flow sets in due to temperature variations, $r_{1,T}$ seems to play the critical role rather than $r_{1,V}$ in deciding x_c. In the present study, the x_c-value is independent of the $A(0)$-value but $x_{m,T}$ - and $x_{m,V}$ -values are dependent upon the $A(0)$-value, as shown in Figure 5. Since the present x_c-value is the invariant for a given Ra_D, it is here called the critical distance to mark the onset of intrinsic instability. The local behavior of the Nusselt number Nu along the streamwise distance x is shown in Figure 6. The present numerical simulation yields the undershoot distance x_u in the plot of Nu versus x, as expected. It is clear that manifest convection exists at $x = x_u$. But the predicted x_u-value is dependent upon the $A(0)$-value like $x_{m,T}$. Here it is shown that $x_{m,T} \cong x_{m,V} \cong x_u$ for a given $A(0)$-value.

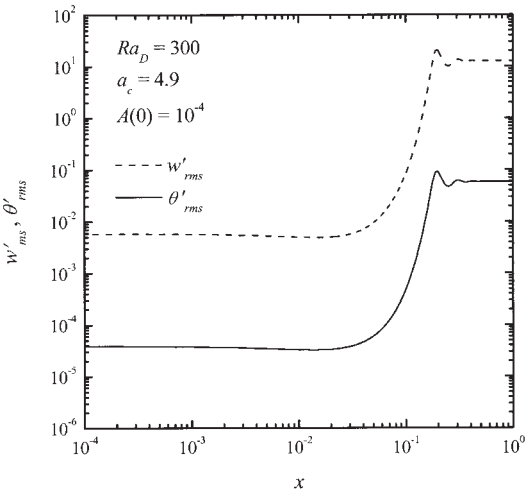

Figure 4. Local behaviors of fluctuations for Ra_D = 300 and a_c = 4.9.

For the present system, Lai and Kulacki[16] observed mixed convection at some downstream distance for various Darcy-Rayleigh and Péclet numbers with variations of heat-source length. They obtained the average Nusselt number $\overline{Nu}$ for a given Ra_D and Pe by measuring the bottom temperature. In the present study their $\overline{Nu}$ corresponds to

$$\overline{Nu} = \frac{1}{x}\int_0^x Nu\,dx. \tag{24}$$

For $Ra_D = 100$ and 300 the local behavior of $\overline{Nu}$ is illustrated in Figure 7. The present results with $A(0) = 10^{-3}$ and 10^{-4} compare well with their experimental data.

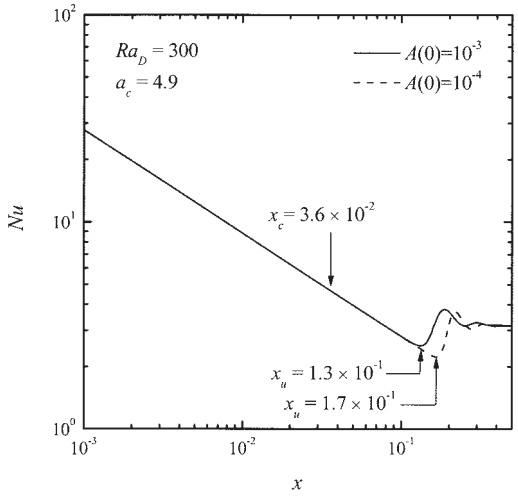

Figure 6. Local behavior of the Nusselt number with $Ra_D = 300$ and $a_c = 4.9$.

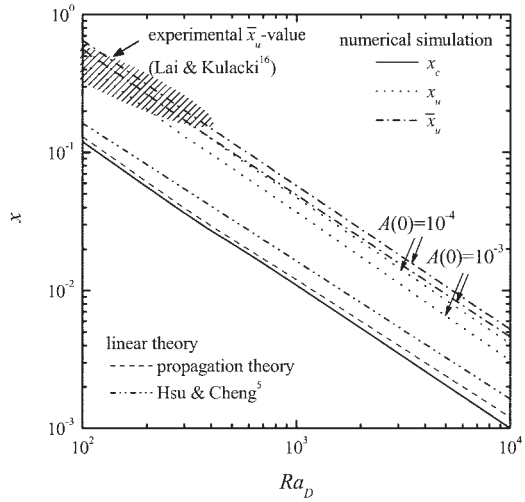

Figure 8. Comparison of predicted characteristic distances with experimental data.

The characteristic distances obtained by the numerical simulation are compared with the previous results in Figure 8. The onset distance of intrinsic instability, $x_{c,}$ is close to the critical distance predicted from the propagation theory, x_c^*. It is shown that the critical distances obtained by Hsu and Cheng[5] are a little larger than the present x_c- and x_c^*-values. They used the bottom boundary condition $\theta_1 = 0$ at $z = 0$ instead of $\partial\theta_1/\partial z = 0$ in Eq. 17a. With the propagation theory, if $\theta_1 = 0$ is used instead of $\partial\theta_1/\partial z = 0$ at $z = 0$ in the boundary condition 17a, the critical conditions are the same as their predictions. For the boundary condition of constant-flux heating systems, $\partial\theta_1/\partial z = 0$ is usually used.[25] It is very interesting that the present numerical predictions are well represented by those from the propagation theory.

The undershoot distance x_u (see Figures 6 and 7) surely ensures the manifestation of secondary flow. In the present simulation, the relations of $x_u \cong 3.6x_c$ and $x_u \cong 4.7x_c$, respectively, for $A(0) = 10^{-3}$ and 10^{-4}, are obtained. It is expected that the instability at $x = x_c$ is extremely small and it should grow until manifest secondary flow is detected. The present numerical results of the undershoot distance of $\overline{Nu}$, $\bar{x}_u$, are compared with experimental data of Lai and Kulacki.[16] The present $\bar{x}_u$-values for $A(0) = 10^{-3}$ and 10^{-4} follow experimental ones to a certain degree. The detection of secondary flow may be connected to $r_{1,V}$ and, therefore, significantly grown rolls would be observed near $x = x_{m,V}(\cong x_u)$. We suppose that the detection distance x_D, at which the first observable motion is detected, exists between x_c and x_u, that is, $x_c \leq x_D \leq x_u(\cong x_{m,V})$ and its exact value is not given explicitly.

For $Ra_D > 10^2$ the numerical critical conditions to mark the onset distance of intrinsic instability are well approximated by

$$Ra_D x_c = 11,\ a_c = 0.28Ra_D^{1/2}, \tag{25}$$

within the error bound of 3%. Here x_c is not sensitive on a near a_c and it is a little smaller than that from the propagation theory (see Eq. 22). It is mentioned that in the Darcy regime the propagation theory yields a good approximation.

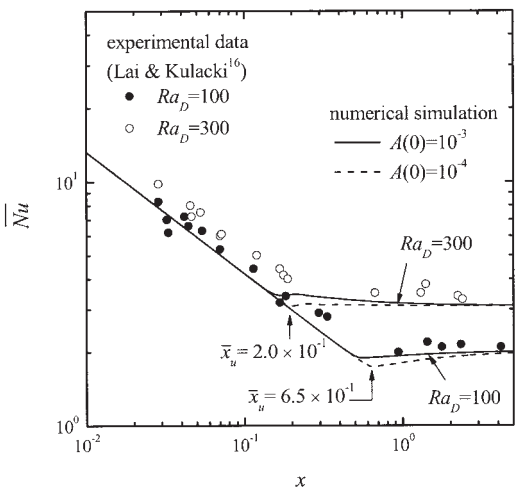

Figure 7. Comparison of the average Nusselt number with available experimental data.

Conclusions

The critical distances to mark the onset of mixed convection in the thermal entrance region of the fluid-saturated porous layer with a laminar primary flow have been investigated based on the propagation theory and also the numerical method. Under the Darcy model, the characteristic distances x_c and x_u have been examined. In the present system, a new stability criterion is suggested such that a fastest growing instability sets in at $x = x_c$ with $r_{1,T} = r_{0,T}$. The numerical results show that the critical distance to mark the onset distance of intrinsic instability, x_c, is the invariant, which is independent of the inlet magnitude of temperature fluctuations, that is, $A(0)$. It is found that the critical distance obtained from the propagation theory is nearly the same as the present x_c-value. It is clear that in the present system linear theory is applied to $x < x_{m,V}$.

The mixed convection is surely observed at the undershoot distance x_u, which is dependent upon the $A(0)$-value. Experimental evidences show that the proper $A(0)$-value may be chosen between 10^{-4} and 10^{-3}. The characteristic distance x_D,

at which the convective motion can be first detected, would be located between x_c and $x_{m,V}$. Therefore, the relation of $x_c \leq x_D \leq x_{m,V} \cong x_u$ is here suggested. The present numerical simulation follows actual phenomena reasonably well for $x_c \leq x \leq x_u$ in comparison with available experimental data and also clarifies the characteristic distances x_c, x_D, and x_u.

Acknowledgments

This work was supported by LG Chemical Ltd., Seoul, under the Brain Korea 21 Project of the Ministry of Education.

Literature Cited

1. Combarnous MA, Bia P. Combined free and forced convection in porous media. *Soc Petroleum Eng J.* 1971;251:399-405.
2. Jones MC, Persichetti JM. Convective instability in packed beds with throughflow. *AIChE J.* 1986;32:1555-1557.
3. Nield DA. Convective instability in porous media with throughflow. *AIChE J.* 1987;33:1222-1224.
4. Homsy GM, Sherwood AE. Convective instability in packed beds with through flow. *AIChE J.* 1976;22:168-174.
5. Hsu CT, Cheng P. Vortex instability of mixed convective flow in a semi-infinite porous medium bounded by a horizontal surface. *Int J Heat Mass Transfer.* 1980;23:789-798.
6. Lee DH, Yoon DY, Choi CK. The onset of vortex instability in laminar natural convection flow over an inclined plate embedded in a porous medium. *Int J Heat Mass Transfer.* 2000;43:2895-2908.
7. Chung TJ, Park JH, Choi CK, Yoon DY. The onset of vortex instability in laminar forced convection flow through a horizontal porous channel. *Int J Heat Mass Transfer.* 2002;45:3061-3064.
8. Kang KH, Choi CK, Hwang IG. Onset of solutal Marangoni convection in a suddenly desorbing liquid layer. *AIChE J.* 2000;46:15-23.
9. Choi CK, Park JH, Kim MC, Lee JD, Kim JJ, Davis EJ. The onset of convective instability in a horizontal fluid layer subjected to a constant heat flux from below. *Int J Heat Mass Transfer.* 2004;47:4377-4384.
10. Hwang IG, Choi CK. Onset of compositional convection during solidification of a two-component melt from a bottom boundary. *J Crystal Growth.* 2004;267:714-723.
11. Park JH, Kim MC, Moon JH, Park SH, Choi CK. The onset of buoyancy-driven convection in a horizontal fluid layer cooled isothermally from above. *IASME Trans*, *Issue 9.* 2005;2:1674-1682.
12. Ihle CF, NiñoY. The onset of nonpenetrative convection in a suddenly cooled layer of fluid. *Int J Heat Mass Transfer.* 2006;49:1442-1451.
13. Riaz A, Hesse M, Tchelepi HA., Orr FM. Onset of convection in a gravitationally unstable diffusive boundary layer in porous media. *J Fluid Mech.* 2006;548:87-111.
14. Kim MC, Chung TJ, Choi CK, The onset of convective instability in the thermal entrance region of plane Poiseuille flow heated uniformly from below. *Int J Heat Mass Transfer.* 2003;46:2629-2636.
15. Choi CK, Chung TJ, Kim MC. Buoyancy effects in plane Couette flow heated uniformly from below with constant heat flux. *Int J Heat Mass Transfer.* 2004;47:2629-2636.
16. Lai FC, Kulacki FA. Experimental study of free and mixed convection in horizontal porous layers locally heated from below. *Int J Heat Mass Transfer.* 1991;34:525-541.
17. Lai FC, Prasad V, Kulacki FA. Effects of the size of heat source on mixed convection in horizontal porous layers heated from below. Proceedings of the 1987 ASME/JSME Thermal Engineering Joint Conference, Vol. 2, Honolulu; 1987:413-419.
18. Prasad V, Lai FC, Kulacki FA. Mixed convection in horizontal porous layers heated from below. *J Heat Transfer.* 1988;110:395-402.
19. Nield DA. Onset of thermohaline convection in a porous medium. *Water Resources Res.* 1968;11:553-560.
20. Ribando RJ, Torrance KE. Natural convection in a porous medium: effects of confinement, variable permeability, and thermal boundary conditions. *J Heat Transfer.* 1976;98:42-48.
21. Choi CK, Park JH, Park HK, Cho HJ, Chung TJ, Kim MC. Temporal evolution of thermal convection in an initially stably-stratified horizontal fluid layer. *Int J Thermal Sci.* 2004;43:817-823.
22. Yang DJ, Choi CK. The onset of thermal convection in a horizontal fluid layer heated from below with time-dependent heat flux. *Phys Fluids.* 2002;14:930-937.
23. Patankar SV. *Numerical Heat Transfer and Fluid Flow.* New York: Hemisphere Pub. Corp.; 1980.
24. Mahler EG, Schechter RS. The stability of a fluid layer with gas absorption. *Chem Eng Sci.* 1970;25:955-968.
25. Nield DA, Bejan A. *Convection in Porous Media.* Berlin: Springer-Verlag; 1992.

Manuscript received July 1, 2005, and revision received Mar. 27, 2006.